Photoinduced Delamination of Metal–Organic Framework Thin Films by Spatioselective Generation of Reactive Oxygen Species

Xiaojing Liu, Antoine Mazel, Stefan Marschner, Zhihua Fu, Marius Muth, Frank Kirschhöfer, Gerald Brenner-Weiss, Stefan Bräse, Stéphane Diring, Fabrice Odobel, Ritesh Haldar,* and Christof Wöll*

ABSTRACT: Metal–organic frameworks (MOFs) built from different building units offer functionalities going far beyond gas storage and separation. In connection with advanced applications, e.g., in optoelectronics, hierarchical MOF on MOF structures fabricated using sophisticated methodologies have recently become particularly attractive. Here, we demonstrate that the structural complexity of MOF based architectures can be further increased by employing highly spatioselective photochemistry. Using a layer by layer, quasi epitaxial synthesis method, we realized a photoactive MOF on MOF hetero bilayer consisting of a porphyrinic bottom layer and a tetraphenylethylene (TPE) based top layer. Illumination of the monolithic thin film with visible light in the presence of oxygen gas results in the generation of reactive oxygen species ($^1O_2$) in the porphyrinic bottom layer, which lead to a photocleavage of the TPE units at the internal interface. We demonstrate that this spatioselective photochemistry can be utilized to delaminate the top layers, yielding two dimensional (2D) MOF sheets with well defined thickness. Experiments using atomic force microscopy (AFM) demonstrate that these platelets can be transferred onto other substrates, thus opening up the possibility of fabricating planar MOF structures using photolithography.

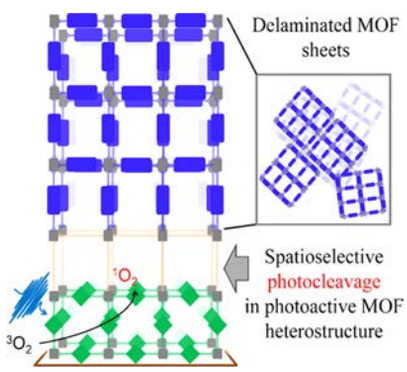

KEYWORDS: *metal–organic frameworks, heterostructure, photochemistry, porphyrin, singlet oxygen*

INTRODUCTION

Functional metal–organic frameworks (MOFs), which are crystalline, porous assemblies of inorganic metal nodes and organic linkers,[1] have gained much attention toward a variety of potential applications, e.g., in the fields of gas capture,[2,3] separation,[4] catalysis,[5,6] and optoelectronics.[7−9] The modular design principle of these reticular networks has created a virtually infinite chemical space, with numerous examples where chemical and physical properties have been tuned in a rational fashion for specific applications.[10] For more advanced applications and device integrations, mesoscopic order and functional synergy on different length scales are now starting to receive attention. To achieve such functional hierarchy, MOF on MOF heterostructures have moved into the focus of research.[11−13] It has been demonstrated that hetero bi or multilayers can be fabricated by growing two different networks with different metal nodes and topology on top of each other. For a number of properties, the heterointerfaces in these MOF on MOF structures introduce the crucial function ality, e.g., photon energy transport and charge separa tion.[11,14−16]

Well defined MOF on MOF heterointerfaces provide phys ical and chemical effects beyond those accessible by the individual MOFs.[17−19] In earlier works, hierarchical MOF on MOF structures were synthesized for particles (e.g., core–shell[20,21]) as well as for planar substrates.[22,23] While MOF on MOF growth has been realized using solvothermal synthesis schemes (multistep synthesis), control over the growth and functionality is not a straightforward process when using this conventional MOF synthesis scheme. Often, individual crystalline facets affect the growth process, giving rise to complications when different facet orientations are ex posed.[24,25] To avoid the complexity of multistep solvothermal processes (where all reactants are present at the same time), liquid phase layer by layer (LBL) methods have been developed.[26] In this approach, the reactants are kept apart, allowing for the programmed assembly of heterostructures. The LBL approach has been successfully used for hetero epitaxy, and even lattice constant mismatches as large as 20% could be overcome.[27,28] The availability of such well defined, crystalline multilayers has allowed us to demonstrate that interesting phenomena occur at such heterointerfaces,

Scheme 1. (a) Schematic Illustration of MOF on MOF Zn PPY TPE Heteroepitaxial Structure Exhibiting Singlet Oxygen ($^1O_2$) Sensitization (Gray Squares = Zinc Paddle Wheel Node, Green = PPY, Orange = TPE); The Structure Includes 30 Cycles of Zn PPY and 20 Cycles of Zn TPE; (b) $^1O_2$ Mediated Oxidation Reaction of TPE and Chemical Structure of the Constituent Linkers

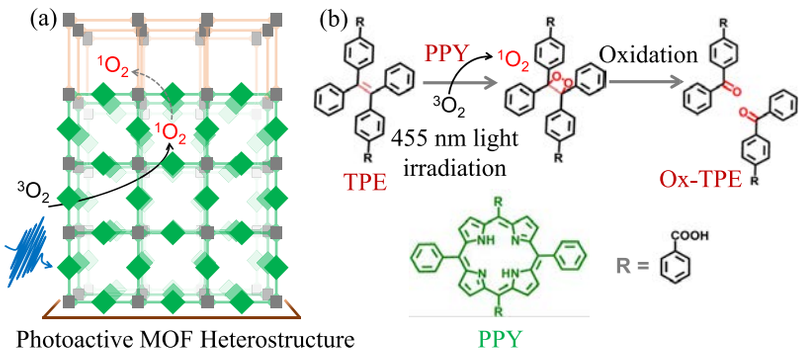

including photon excitation and charge carrier transport.[29,30] To further explore the potential of MOF on MOF hetero structures, we examined photochemically active MOF on MOF heterostructures to realize spatial control of photo chemical reactions. For this purpose, we designed a heterostructure combining a photosensitizer and a reactant. We were able to demonstrate that photoinduced reactions only take place at the well defined crystalline interface between the different materials, allowing an unprecedented photochemical reaction at the MOF on MOF interface, as illustrated in Scheme 1.

To implement photochemical activity in the heterostructure, we explored the well known singlet oxygen ($^1O_2$) oxidation chemistry.[31] $^1O_2$ is a reactive oxidizing agent, which can be generated by activation of $^3O_2$ using a photosensitizer. We exploit the $^1O_2$ by reacting it with olefins (e.g., stilbene) to form a dioxetane intermediate, which then converts into the final oxidation product, such as a ketone or an aldehyde.[32] When carrying out this reaction in solution, reactivities often vary strongly due to quenching of the reactive $^1O_2$ species.[33] Additionally, reaction kinetics in solution and in the solid state are slowed down because of the hindered diffusion of $^1O_2$. To overcome these limitations, we used a porous crystalline array of porphyrins as a photosensitizer and tetraphenylethylene as a reactant to construct photoactive MOF on MOF heterostruc ture (Scheme 1b).

We used a LBL, liquid phase epitaxy (LPE) method of depositing the oriented, crystalline MOF structure on a desired surface to fabricate the MOF on MOF heterostructure as a monolithic, surface anchored MOF (SURMOF). We chose a SURMOF 2 variant, a two dimensional (2D) layered structure constructed by tethering paddle wheel type secondary building units (metal oxo nodes) with a ditopic organic linker (chromophore).[34] The photosensitizer and reactive MOF layers were synthesized using a ditopic porphyrin based linker (PPY) and substituted tetraphenylethylene (TPE) linker, respectively. Visible light excitation of the PPY MOF layer of the PPY TPE heterolayered SURMOF sensitizes $^3O_2$ to $^1O_2$; subsequently, the reactive $^1O_2$ diffuses to the neighboring TPE MOF layer to oxidize −C═C− of TPE. This facile photochemical oxidation process cleaves the TPE linker and disrupts the MOF structure, as the MOF is constituted by tethering TPE and the paddle wheel secondary building unit. In the following, we demonstrate the *de novo* photoactive heterolayer design approach toward facile interfacial photo oxidation and its application toward core substituted naph thalenediimide (cNDI) based nanostructure synthesis by designing a new hetero multilayer SURMOF structure. In recent years, the exfoliation of bulk 2D MOF crystallites to yield nanosheets with thicknesses of a few layers has attracted much attention, and successful strategies, e.g., based on sonication, have been reported.[33,35] The method proposed here carries the advantage that it can be applied to planar substrates and that it can, in principle, be combined with photolithography.

RESULTS AND DISCUSSION

To realize a solvent independent reaction platform, a bespoke MOF material provides an ideal selection because it offers a well defined, modular chemical environment. The combinato rial advantages, such as the precise local structure information, easy inclusion of diverse photoactive chromophores as a linker, and fixed spatial geometry of the linker node, have allowed the use of MOFs for exploring various photophysical processes and chemical reactions. In previous applications of porphyrin based porous MOFs for selective oxidation reactions, it was realized that excitation of the $^3O_2$ oxygen is facile at ambient temperature.[36] These earlier works have also shown that the presence of the MOF metal nodes does not interfere with the $^1O_2$ deactivation/activation process. Note that, previously, the generation of the reactive oxygen species by a crystalline PPY based MOF or polymer has been demonstrated, but the photochemical reaction (oxidation) has been performed in the presence of a solvent, giving rise to several competing reactions, as mentioned above.

To avoid any solvent induced effects (including unwanted quenching), we utilized the LPE method[26] to construct a SURMOF 2[32] type of structure, formed by connecting a Zn based paddle wheel type secondary building unit and two ditopic organic linkers, PPY[36] and TPE.[37] This node−linker combination creates a square grid like 2D structure, with the 2D sheets stacked such as to yield a crystalline layer with a *P*4 symmetry. As shown in Figure S1, the 2D sheets are oriented parallel to the substrate plane (along [010] direction), with van der Waals interactions providing the intersheet coupling. To construct the proposed crystalline heterointerface between Zn TPE and Zn PPY, the first 30 cycles of Zn PPY and then 20 cycles of Zn TPE were deposited by the LBL spin coating method[38] on precleaned quartz glass and Si/SiO_2 substrates. A lattice mismatch of ~7% among the two structures (2.4 and 2.6

nm) did not affect the heteroepitaxial growth, as revealed from the out of plane X ray diffraction (XRD) data recorded for this bilayer structure (Figure 1).

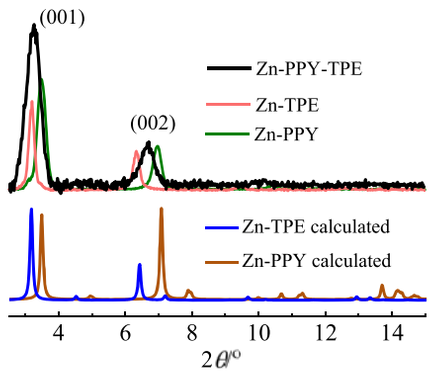

Figure 1. Out of plane X ray diffraction patterns of Zn PPY, Zn TPE, MOF on MOF structure Zn PPY TPE, and the simulated Zn PPY and Zn TPE.

Before testing the photosensitization process in the heterolayer MOF, we monitored the reactivity of TPE linkers in a TPE/PPY linker mixture solvated in ethanol. Although in this mixture, sensitizing PPY linkers are present, irradiation with 455 nm light did not result in the TPE linker oxidation, as revealed by the ultraviolet−visible (UV−vis) spectra (Figure 2a) recorded before and after illumination. The absence of oxidation products was corroborated by a liquid chromatog raphy−mass spectrometry (LC−MS) analysis, where no oxidation product of the TPE linker could be detected (Figure S2). We attribute this finding to the fast quenching of the reactive $^1O_2$ species by the solvent molecules.

In contrast, at the solvent free TPE/PPY MOF on MOF heterointerface, such a reaction could be clearly observed. The UV−vis spectra of this bilayer recorded before and after irradiation with 455 nm light in the presence of O_2 clearly revealed a decrease in absorption at ∼350 nm, which is related to the consumption of Zn TPE (Figure 2b). Note that no such changes occurred in the absence of O_2 (Figure 2b). To identify the chemical change in the bilayer, we carried out an LC−MS experiment of the digested SURMOF (dissolved by 5% acetic acid in ethanol). The chromatogram clearly showed a new peak, which can be assigned to the TPE oxidation product (Ox TPE; $[M - H]^-$ = 301.088 Da; PPY is detected in positive mode as $[M + H]^+$ = 701.218 Da; Figures 2c and S3). These observations clearly demonstrate that the oxidation process in the crystalline state is comparatively facile. Obviously, the photogenerated $^1O_2$ is able to reach the TPE linkers, whereas in solution state this reaction is hindered by quick quenching of the reactive oxygen species. As can be seen from the LC−MS profile in Figure 2c, not all of the TPE molecules are oxidized. We tentatively relate this observation either to a $^1O_2$ diffusion barrier across the MOF/MOF heterointerface or to a rapid quenching of the $^1O_2$ species inside the TPE SURMOF structure.

After establishing the photochemical oxidation process in the crystalline form of the heterostructure PPY TPE, we applied this light mediated process to delaminate a MOF layer deposited on top of the photoactive bilayer. To this end, we chose a core substituted naphthalenediimide (cNDI)[11] based ditopic linker to construct an isoreticular Zn SURMOF 2 as the top layer (Figures 3a, S4, and S5). Although the lattice parameters of Zn cNDI and Zn TPE differed by ∼7% (2.4 and 2.64 nm), an oriented, crystalline trilayer structure (Zn PPY TPE cNDI) was formed, as demonstrated by the XRD data shown in Figure 3a. To perform the light mediated detachment

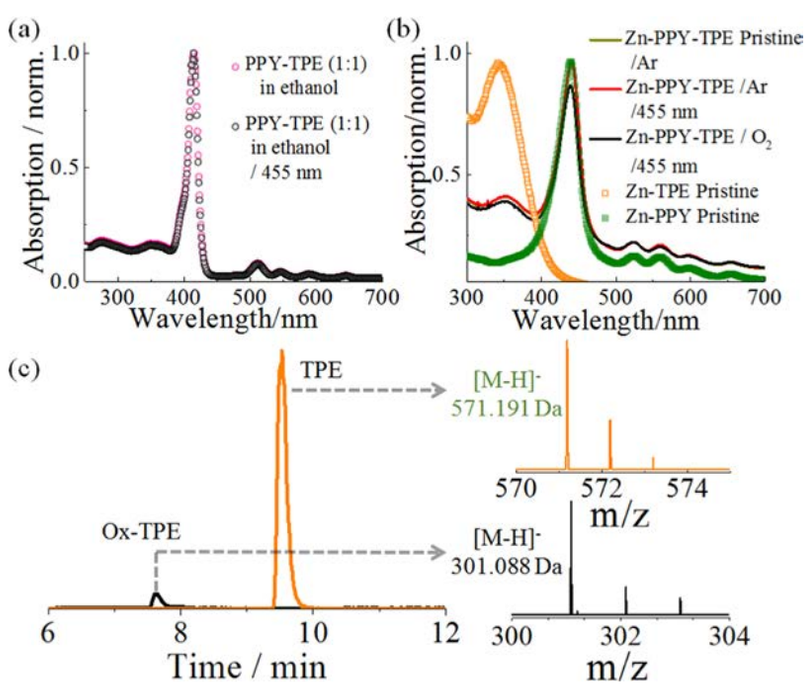

Figure 2. (a) UV−vis spectra of PPY and TPE linkers (1:1) in ethanol before and after 455 nm light irradiation; (b) UV−vis spectra of Zn PPY, Zn TPE, and Zn PPY TPE in different conditions: pristine, 455 nm irradiation in an Ar and O_2 atmosphere; (c) LC−MS profile of the dissolved heterostructure (Zn PPY TPE) in negative ion mode and the isotopic mass distribution of TPE (orange) and its oxidized product (black). The two peaks in orange are attributed to the isotopic compositions of TPE with identical mass.

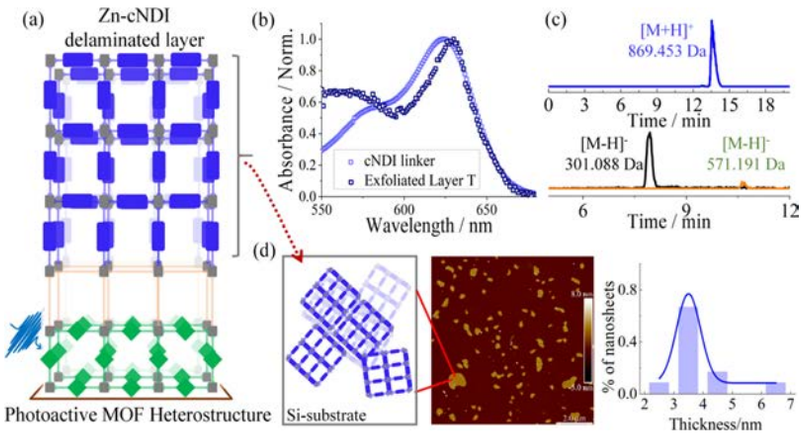

Figure 3. (a) Illustration of the top Zn cNDI (blue) epitaxially grown on the Zn PPY TPE layer; (b) UV−vis spectra of the cNDI linker and the delaminated Zn cNDI layer in ethanol; (c) LC−MS profiles of the delaminated Zn cNDI top layer (dissolved by 5% acetic acid in ethanol) in negative and positive ion modes showing the characteristic m/z of TPE (orange), Ox TPE (black), and cNDI (blue); (retention times of TPE and Ox TPE are dependent on the polarity of columns) (d) left: schematic illustration of delaminated Zn cNDI layers transferred on the Si substrate, middle: AFM image of the delaminated Zn cNDI 2D layers, and right: distribution of the nanosheet (>30) thicknesses observed in two sets of experiments carried out in similar processes.

process of the upper MOF layer, we carried out the following steps (Figure S6): (a) deposition of the Zn cNDI layer on top of the Zn PPY TPE by spin coating (120 cycles, thickness ∼120 nm estimated by ellipsometry); (b) sealing the trilayer structure on the SiO_2 substrate (1×1 cm^2 size) in an oxygen filled glass tube, (c) irradiation with 455 nm light for ∼6 h; (d) removal of the top (delaminated) cNDI MOF layer by first drop casting of ∼100 μL on the film and leaving it undisturbed for ∼1 min. Subsequently, a flat, precleaned Si substrate was gently pressed onto the dispersion obtained in step (d). Atomic force microscopy (AFM, see below) was then used to study the substrates. For other spectroscopic and LC−MS characterizations, we just rinsed the trilayer with ethanol (∼100 μL), and the rinsing solution was analyzed.

After rinsing with ethanol, the trilayer MOF film exhibited a distinct decrease in the absorption maximum at ∼620 nm, which is the characteristic excitation of Zn cNDI (Figure S7). This observation indicates the detachment of the Zn cNDI layer from the trilayer structure. The rinsing solution was probed by UV−vis absorption measurement, which showed a characteristic absorption maximum of cNDI, supporting the postulated light mediated detachment process (Figure 3b). Further, by the LC−MS experiment of the 5% acetic acid/ethanol treated rinsing solution, we could identify the characteristic m/z of cNDI (in positive mode as $[M + H]^+$ = 869.453 Da; Figures 3c and S8). We could also detect the Ox TPE as a major product (compared to unreacted TPE) in the same rinsing solution in negative ion mode (Figure 3c). These observations supported the hypothesis that the top Zn cNDI layer was delaminated by photochemical reaction.

The most direct evidence for successful delamination comes from AFM measurement on flat substrates onto which the delaminated parts of the SURMOF have been transferred (see Figure S6). We could clearly observe flat sheet like structures with an average thickness of ∼3.6 nm and regular shaped edges (Figure 3d), with diameters ranging between large (>1 μm) to small (∼50 nm). The thicknesses of the sheets correspond to three stacked 2D layers of Zn cNDI, lying flat on the Si substrate, as illustrated in Figure 3d. This observation indicates that after the photo oxidation triggered delamination process in ethanol, the stacked Zn cNDI 2D layers are delaminated to yield stacked 2D structures of homogeneous thickness and different diameters.

CONCLUSIONS

In conclusion, a MOF on MOF heterostructure has been designed and it allows delaminating the top MOF layer through oxidative linker cleavage. The reactive oxygen species driving this reaction are generated in a porphyrin MOF bottom layer and diffuse to the top layer to react with a TPE linker MOF. The oxidative linker cleavage at the interface leads to delamination of the final top layer MOF. A comparison with the same reaction taking place in the corresponding mixture of linkers in solution reveals that the porous, crystalline arrangement of the reactants is very beneficial: on one hand, the quenching of $^1O_2$ by solvent molecules is suppressed, and on the other hand, the porosity of the frameworks allows the photogenerated reactive oxygen species to reach the TPE linkers. This method of 2D nanostructure delamination driven by photochemistry can also be applied to other MOF heterolayers. In addition, using photolithography should be possible, which will allow us to more accurately define the shape of the delaminated particles.

AUTHOR INFORMATION

Corresponding Authors

Ritesh Haldar − *Karlsruhe Institute of Technology (KIT), Institute of Functional Interfaces (IFG), 76344 Eggenstein Leopoldshafen, Germany; Tata Institute of Fundamental Research Hyderabad, Hyderabad 500046 Telangana, India;*

orcid.org/0000 0001 9697 9169; Email: riteshhaldar@tifrh.res.in

Christof Wöll − *Karlsruhe Institute of Technology (KIT), Institute of Functional Interfaces (IFG), 76344 Eggenstein Leopoldshafen, Germany;* orcid.org/0000 0003 1078 3304; Email: christof.woell@kit.edu

Authors

Xiaojing Liu − *Karlsruhe Institute of Technology (KIT), Institute of Functional Interfaces (IFG), 76344 Eggenstein Leopoldshafen, Germany*

Antoine Mazel − *Université de Nantes, CNRS, CEISAM UMR 6230, F 44000 Nantes, France*

Stefan Marschner − *Karlsruhe Institute of Technology (KIT), Institute of Organic Chemistry (IOC), 76131 Karlsruhe, Germany*

Zhihua Fu − *Karlsruhe Institute of Technology (KIT), Institute of Functional Interfaces (IFG), 76344 Eggenstein Leopoldshafen, Germany*

Marius Muth − *Karlsruhe Institute of Technology (KIT), Institute of Functional Interfaces (IFG), 76344 Eggenstein Leopoldshafen, Germany*

Frank Kirschhöfer − *Karlsruhe Institute of Technology (KIT), Institute of Functional Interfaces (IFG), 76344 Eggenstein Leopoldshafen, Germany*

Gerald Brenner Weiss − *Karlsruhe Institute of Technology (KIT), Institute of Functional Interfaces (IFG), 76344 Eggenstein Leopoldshafen, Germany*

Stefan Bräse − *Karlsruhe Institute of Technology (KIT), Institute of Organic Chemistry (IOC), 76131 Karlsruhe, Germany; Karlsruhe Institute of Technology (KIT), Institute of Biological and Chemical Systems (IBCS FMS), 76344 Eggenstein Leopoldshafen, Germany;* orcid.org/0000 0003 4845 3191

Stéphane Diring − *Université de Nantes, CNRS, CEISAM UMR 6230, F 44000 Nantes, France*

Fabrice Odobel − *Université de Nantes, CNRS, CEISAM UMR 6230, F 44000 Nantes, France;* orcid.org/0000 0001 7289 4160

ACKNOWLEDGMENTS

X.L., R.H., S.B., and C.W. acknowledge support from the Deutsche Forschungsgemeinschaft (DFG, German Research Foundation) under the Germany Excellence Strategy via the Excellence Cluster 3D Matter Made to Order (grant no. EXC 2082/1 390761711). S.B. and C.W. thank DFG also for support in the context of the priority program COORNETs (SPP 1928). A.M., S.D., and F.O. acknowledge Région des Pays de la Loire through the program LUMOMAT for the financial support of this research with the project LumoMOF. S.D. is grateful for financial support from ANR PhotoMOF project, Grant ANR 18 CE05 0008 01.

REFERENCES

(1) Kitagawa, S.; Kitaura, R.; Noro, S. i. Functional Porous Coordination Polymers. *Angew. Chem., Int. Ed.* **2004**, *43*, 2334−2375.

(2) Ahmed, A.; Seth, S.; Purewal, J.; Wong Foy, A. G.; Veenstra, M.; Matzger, A. J.; Siegel, D. J. Exceptional Hydrogen Storage Achieved by Screening Nearly Half a Million Metal Organic Frameworks. *Nat. Commun.* **2019**, *10*, No. 1568.

(3) Ding, M.; Flaig, R. W.; Jiang, H. L.; Yaghi, O. M. Carbon Capture and Conversion Using Metal−Organic Frameworks and MOF based Materials. *Chem. Soc. Rev.* **2019**, *48*, 2783−2828.

(4) Qian, Q.; Asinger, P. A.; Lee, M. J.; Han, G.; Mizrahi Rodriguez, K.; Lin, S.; Benedetti, F. M.; Wu, A. X.; Chi, W. S.; Smith, Z. P. MOF Based Membranes for Gas Separations. *Chem. Rev.* **2020**, *120*, 8161−8266.

(5) Yang, D.; Gates, B. C. Catalysis by Metal Organic Frameworks: Perspective and Suggestions for Future Research. *ACS Catal.* **2019**, *9*, 1779−1798.

(6) Pascanu, V.; González Miera, G.; Inge, A. K.; Martín Matute, Bn. Metal−Organic Frameworks as Catalysts for Organic Synthesis: a critical perspective. *J. Am. Chem. Soc.* **2019**, *141*, 7223−7234.

(7) Xie, L. S.; Skorupskii, G.; Dincă, M. Electrically Conductive Metal−Organic Frameworks. *Chem. Rev.* **2020**, *120*, 8536−8580.

(8) Allendorf, M. D.; Dong, R.; Feng, X.; Kaskel, S.; Matoga, D.; Stavila, V. Electronic Devices Using Open Framework Materials. *Chem. Rev.* **2020**, *120*, 8581−8640.

(9) Haldar, R.; Jakoby, M.; Kozlowska, M.; Rahman Khan, M.; Chen, H.; Pramudya, Y.; Richards, B. S.; Heinke, L.; Wenzel, W.; Odobel, F.; Diring, S.; Howard, I. A.; Lemmer, U.; Wöll, C. Tuning Optical Properties by Controlled Aggregation: Electroluminescence Assisted by Thermally Activated Delayed Fluorescence from Thin Films of Crystalline Chromophores. *Chem. Eur. J.* **2020**, *26*, 17016−17020.

(10) Furukawa, H.; Cordova, K. E.; O'Keeffe, M.; Yaghi, O. M. The Chemistry and Applications of Metal Organic Frameworks. *Science* **2013**, *341*, No. 1230444.

(11) Haldar, R.; Wöll, C. Hierarchical Assemblies of Molecular Frameworks—MOF on MOF Epitaxial Heterostructures. *Nano Res.* **2021**, *14*, 355−368.

(12) Chai, L.; Pan, J.; Hu, Y.; Qian, J.; Hong, M. Rational Design and Growth of MOF on MOF Heterostructures. *Small* **2021**, *17*, No. 2100607.

(13) Ikigaki, K.; Okada, K.; Tokudome, Y.; Toyao, T.; Falcaro, P.; Doonan, C. J.; Takahashi, M. MOF on MOF: Oriented Growth of Multiple Layered Thin Films of Metal−Organic Frameworks. *Angew. Chem.* **2019**, *131*, 6960−6964.

(14) Haldar, R.; Chen, H.; Mazel, A.; Chen, D. H.; Gupta, G.; Dua, N.; Diring, S.; Odobel, F.; Wöll, C. Antenna Doping: The Key for Achieving Efficient Optical Wavelength Conversion in Crystalline Chromophoric Heterolayers. *Adv. Mater. Interfaces* **2021**, *8*, No. 2100262.

(15) Oldenburg, M.; Turshatov, A.; Busko, D.; Wollgarten, S.; Adams, M.; Baroni, N.; Welle, A.; Redel, E.; Wöll, C.; Richards, B. S.; Howard, I. A. Photon Upconversion at Crystalline Organic−Organic Heterojunctions. *Adv. Mater.* **2016**, *28*, 8477−8482.

(16) Knebel, A.; Wulfert Holzmann, P.; Friebe, S.; Pavel, J.; Strauß, I.; Mundstock, A.; Steinbach, F.; Caro, J. Hierarchical Nanostructures of Metal Organic Frameworks Applied in Gas Separating ZIF 8 on ZIF 67 Membranes. *Chem. Eur. J.* **2018**, *24*, 5728−5733.

(17) Chen, D. H.; Haldar, R.; Neumeier, B. L.; Fu, Z. H.; Feldmann, C.; Wöll, C.; Redel, E. Tunable Emission in Heteroepitaxial Ln SURMOFs. *Adv. Funct. Mater.* **2019**, *29*, No. 1903086.

(18) Chandresh, A.; Liu, X.; Wöll, C.; Heinke, L. Programmed Molecular Assembly of Abrupt Crystalline Organic/Organic Hetero interfaces Yielding Metal Organic Framework Diodes with Large On Off Ratios. *Adv. Sci.* **2021**, *8*, No. 2001884.

(19) Zhu, K.; Fan, R.; Wu, J.; Wang, B.; Lu, H.; Zheng, X.; Sun, T.; Gai, S.; Zhou, X.; Yang, Y. MOF on MOF Membrane with Cascading Functionality for Capturing Dichromate Ions and p Arsanilic Acid Turn On Sensing. *ACS Appl. Mater. Interfaces* **2020**, *12*, 58239−58251.

(20) Son, J.; Lee, H. J.; Oh, M. Systematic Formation of Multilayered Core−Shell Microspheres through the Multistep Growth of Coordination Polymers. *Chem. Eur. J.* **2013**, *19*, 6546−6550.

(21) Koh, K.; Wong Foy, A. G.; Matzger, A. J. MOF@ MOF: microporous core−shell architectures. *Chem. Commun.* **2009**, 6162−6164.
(22) Lee, H. J.; Cho, Y. J.; Cho, W.; Oh, M. Controlled Isotropic or Anisotropic Nanoscale Growth of Coordination Polymers: Formation of Hybrid Coordination Polymer Particles. *ACS Nano* **2013**, *7*, 491−499.
(23) Kwon, O.; Kim, J. Y.; Park, S.; Lee, J. H.; Ha, J.; Park, H.; Moon, H. R.; Kim, J. Computer aided Discovery of Connected Metal Organic Frameworks. *Nat. Commun.* **2019**, *10*, No. 3620.
(24) Ha, J.; Moon, H. R. Synthesis of MOF on MOF Architectures in the Context of Interfacial Lattice Matching. *CrystEngComm* **2021**, *23*, 2337−2354.
(25) Liu, C.; Sun, Q.; Lin, L.; Wang, J.; Zhang, C.; Xia, C.; Bao, T.; Wan, J.; Huang, R.; Zou, J. Ternary MOF on MOF Heterostructures with Controllable Architectural and Compositional Complexity via Multiple Selective Assembly. *Nat. Commun.* **2020**, *11*, No. 4971.
(26) Shekhah, O.; Wang, H.; Kowarik, S.; Schreiber, F.; Paulus, M.; Tolan, M.; Sternemann, C.; Evers, F.; Zacher, D.; Fischer, R. A.; Wöll, C. Step by Step Route for the Synthesis of Metal−Organic Frameworks. *J. Am. Chem. Soc.* **2007**, *129*, 15118−15119.
(27) Wang, Z.; Liu, J.; Lukose, B.; Gu, Z.; Weidler, P. G.; Gliemann, H.; Heine, T.; Wöll, C. Nanoporous Designer Solids with Huge Lattice Constant Gradients: Multiheteroepitaxy of Metal−Organic Frameworks. *Nano Lett.* **2014**, *14*, 1526−1529.
(28) Shekhah, O.; Hirai, K.; Wang, H.; Uehara, H.; Kondo, M.; Diring, S.; Zacher, D.; Fischer, R. A.; Sakata, O.; Kitagawa, S.; Furukawa, S.; Wöll, C. MOF on MOF heteroepitaxy: perfectly oriented [Zn2(ndc)2(dabco)]n grown on [Cu2(ndc)2(dabco)]n thin films. *Dalton Trans.* **2011**, *40*, 4954−4958.
(29) Ogilby, P. R. Singlet Oxygen: there is indeed something new under the sun. *Chem. Soc. Rev.* **2010**, *39*, 3181−3209.
(30) da Hora Machado, A. E.; de Andrade, M. L.; Severino, D. Oxidation of an Electron rich Olefin Induced by Singlet Oxygen: mechanism for tetraphenylethylene. *J. Photochem. Photobiol., A* **1995**, *91*, 179−185.
(31) Bregnhøj, M.; Westberg, M.; Jensen, F.; Ogilby, P. R. Solvent dependent Singlet Oxygen Lifetimes: temperature effects implicate tunneling and charge transfer interactions. *Phys. Chem. Chem. Phys.* **2016**, *18*, 22946−22961.
(32) Liu, J.; Lukose, B.; Shekhah, O.; Arslan, H. K.; Weidler, P.; Gliemann, H.; Bräse, S.; Grosjean, S.; Godt, A.; Feng, X.; Müllen, K.; Magdau, I. B.; Heine, T.; Wöll, C. A Novel Series of Isoreticular Metal Organic Frameworks: realizing metastable structures by liquid phase epitaxy. *Sci. Rep.* **2012**, *2*, No. 921.
(33) Sang, X.; Liu, D.; Song, J.; Wang, C.; Nie, X.; Shi, G.; Xia, X.; Ni, C.; Wang, D. High efficient Liquid Exfoliation of 2D Metal Organic Framework using deep eutectic solvents. *Ultrason. Sonochem.* **2021**, *72*, No. 105461.
(34) Luo, Y. H.; Chen, C.; He, C.; Zhu, Y. Y.; Hong, D. L.; He, X. T.; An, P. J.; Wu, H. S.; Sun, B. W. Single Layered Two Dimensional Metal−Organic Framework Nanosheets as an in Situ Visual Test Paper for Solvents. *ACS Appl. Mater. Interfaces* **2018**, *10*, 28860−28867.
(35) Chen, Y. Z.; Wang, Z. U.; Wang, H.; Lu, J.; Yu, S. H.; Jiang, H. L. Singlet Oxygen Engaged Selective Photo Oxidation over Pt Nanocrystals/Porphyrinic MOF: The Roles of Photothermal Effect and Pt Electronic State. *J. Am. Chem. Soc.* **2017**, *139*, 2035−2044.
(36) Liu, J.; Zhou, W.; Liu, J.; Howard, I.; Kilibarda, G.; Schlabach, S.; Coupry, D.; Addicoat, M.; Yoneda, S.; Tsutsui, Y.; Sakurai, T.; Seki, S.; Wang, Z.; Lindemann, P.; Redel, E.; Heine, T.; Wöll, C. Photoinduced Charge Carrier Generation in Epitaxial MOF Thin Films: High Efficiency as a Result of an Indirect Electronic Band Gap? *Angew. Chem., Int. Ed.* **2015**, *54*, 7441−7445.
(37) Haldar, R.; Diring, S.; Samanta, P. K.; Muth, M.; Clancy, W.; Mazel, A.; Schlabach, S.; Kirschhöfer, F.; Brenner Weiß, G.; Pati, S. K.; Odobel, F.; Wöll, C. Enhancing Selectivity and Kinetics in Oxidative Photocyclization by Supramolecular Control. *Angew. Chem., Int. Ed.* **2018**, *57*, 13662−13665.
(38) Haldar, R.; Jakoby, M.; Mazel, A.; Zhang, Q.; Welle, A.; Mohamed, T.; Krolla, P.; Wenzel, W.; Diring, S.; Odobel, F.; et al. Anisotropic energy transfer in crystalline chromophore assemblies. *Nat. Commun.* **2018**, *9*, No. 4332.